



# Pupil steerable Maxwellian AR display with gaze matching

Junyu Zou, SID Student Member  | Zhenyi Luo, SID Student Member |  
Shin-Tson Wu, SID Fellow 

College of Optics and Photonics,  
University of Central Florida, Orlando,  
Florida, USA

## Correspondence

Shin-Tson Wu, College of Optics and  
Photonics, University of Central Florida,  
Orlando, FL 32816, USA.  
Email: swu@creol.ucf.edu

## Funding information

Goertek Electronics

## Abstract

We demonstrate a gaze-matched Maxwellian-view augmented reality (AR) system with an enlarged eyebox. Three viewpoints are generated by three cholesteric liquid crystal (CLC) off-axis lenses, respectively. The location, diameter, and diffraction angle of these CLC lenses are designed so that the chief rays of each viewpoint match with the corresponding gaze directions. The CLC lenses have a high diffraction efficiency (up to 98%), large off-axis angle ( $60^\circ$ ), and small  $f$ -number, which contributes to the  $55^\circ$  central field of view. Such an AR system exhibits several attractive features for practical applications, including aberration-free, high optical efficiency, high transmittance for the ambient light, relatively large field of view, compact size, and lightweight.

## KEYWORDS

augmented reality, cholesteric liquid crystal lens, gaze matching, large diffraction angel, Maxwellian-view display, pupil steering

## 1 | INTRODUCTION

The Maxwellian display system was applied to virtual reality (VR) in early 1990s because of its high brightness and potentially wide field of view (FOV).<sup>1</sup> Since the development of holographic optical elements (HOEs), the Maxwellian view was integrated in AR systems in late 1990s.<sup>2,3</sup> Laser projector and lens coupler are the key components in a typical Maxwellian AR system, in which the lens focal point should be located at the center of the observer's pupil. In principle, all the light from the optical engine will enter the pupil; thus, it can achieve a very high efficiency and small form factor. Moreover, since the focal point is located at the center of pupil, the pupil lens will not introduce any focal power to the signal so that Maxwellian systems will not suffer from the vergence–accommodation conflict (VAC) issue.<sup>4,5</sup> However, the most significant drawback of Maxwellian system is its small eyebox. Several approaches have been proposed to enlarge the eyebox, and they can be classified

into two groups: pupil duplication (Figure 1A)<sup>6–8</sup> and pupil steering (Figure 1B).<sup>9–12</sup>

In Figure 1A, pupil duplication aims to split the collimated beam into multiple directions by using a HOE,<sup>6,13</sup> beam splitter array,<sup>7</sup> or spatial light modulator (SLM),<sup>8</sup> and each direction corresponds to one viewpoint. This approach does not require an eye-tracking system, so it is cost effective, but it will introduce some problems. The most significant one is that the space gap between two adjacent viewpoints could be too large (Figure 2A) or too small (Figure 2B). Because all the viewpoints appear simultaneously, the observer will see no imaging or partial imaging when the eyeball rotates to the middle of two viewpoints. Another problem is illustrated in Figure 2C. Except for the central viewpoint, the direction of chief ray and the user's viewing direction (eye gaze) will not be matched. This gaze mismatching will introduce unnatural image and annoying viewing experience at these viewpoints.<sup>14,15</sup> Moreover, all the viewpoints appear simultaneously, but

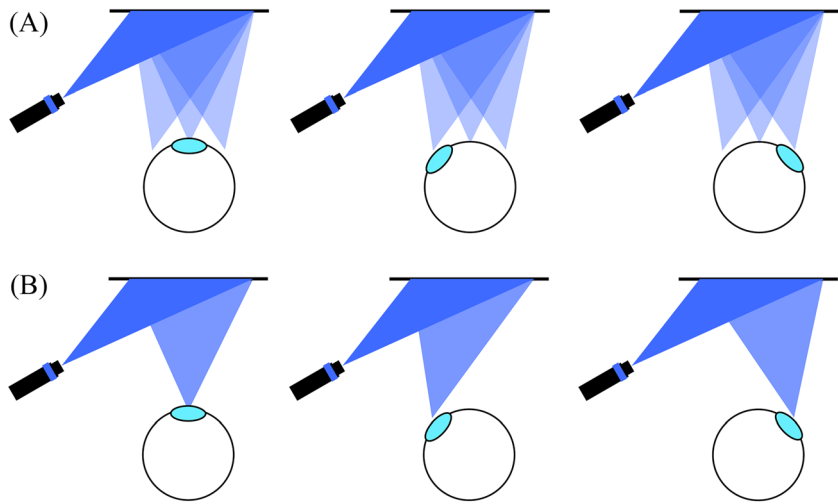


**FIGURE 1** Schematic of Maxwellian-view system with an extended eyebox based on (A) pupil duplication and (B) pupil steering

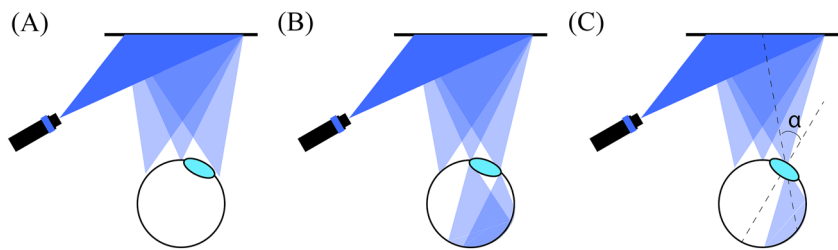


**FIGURE 2** Problems in the pupil duplication method: the distance between two viewpoints is (A) too large and (B) too small; (C) mismatch between the viewing direction (eye gaze) and chief ray

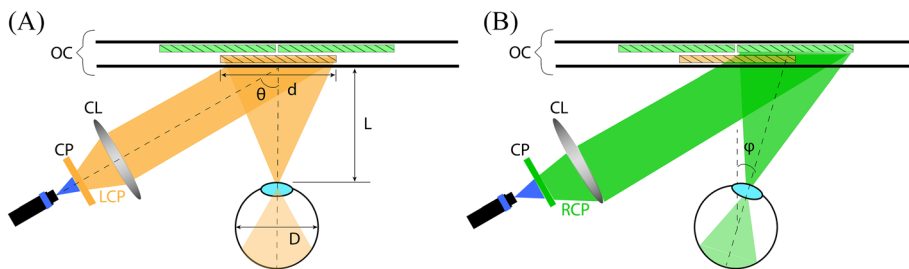


**FIGURE 3** The schematic of the proposed pupil steering system with (A) LCP and (B) RCP input. CL, collimating lens; CP, circular polarizer; OC, optical combiner

only one is used at a time. Therefore, the optical efficiency of pupil duplication will drop to  $1/N$ , if  $N$  viewpoints are generated.

In contrast, the pupil steering approach only presents one viewpoint, so it can prevent the first and third shortcomings mentioned above, but the mismatching between the chief ray and eye gaze still exists. Moreover, the pupil steering system requires an eye tracking and a beam steering device to accommodate the eye rotation. On the other hand, it is difficult to obtain a lens coupler that can achieve diffraction limitation at multiple incident angles, and the imaging quality at some viewpoints will drop significantly.<sup>10</sup> Therefore, there is an urgent need to develop a Maxwellian-view AR system with expanded eyebox, natural viewing experience, good imaging quality, high optical efficiency, and high ambient light transmittance while keeping the system simple, compact, and lightweight.

In this paper, we present a new pupil steering Maxwellian-view AR system structure, which can satisfy all the requirements mentioned above. This system using polarization selective off-axis cholesteric liquid crystal (CLC) lens array as the optical combiner, and each lens corresponds to one viewpoint. The diffraction angle, lens profile, and location of each lens can be customized. In this design, the imaging quality and viewing experience can be optimized for each viewpoint.

## 2 | SYSTEM CONFIGURATION AND SIMULATION

The schematic of the proposed AR system is shown in Figure 3. The light engine is a laser projector. The circular polarizer (CP) can convert the projected beam to either left- or right-handed circularly polarized

(LCP/RCP) light; then it will be collimated by a collimation lens (CL) before reaching the optical combiner. In the design, the LCP/RCP inputs have the same input angles, which match the off-axis angles of the CLC lenses. The optical combiner is comprised of two-layer off-axis CLC lens arrays (here we just use three lenses to prove concept). The lenses on each layer have the chirality working for one kind of circular polarized light. These off-axis CLC lenses have the focal points located on the surface of the eyeball, but corresponding to different gaze directions. In this work, we create three viewpoints corresponding to  $0^\circ$ ,  $+16^\circ$ , and  $-16^\circ$  gaze directions ( $\varphi$ ). The diameter of the eyeball ( $D$ ) is set to be 24 mm. The

off-axis angle of the CLC lens ( $\theta$ ) is designed to be  $60^\circ$ , which is large, and the input beam will not be blocked by the eyeball. In such a system configuration, the phase profile of each off-axis liquid crystal lens is recorded independently so that the optical aberration can be minimized.

In Figure 3A, the lens diameter ( $d$ ) and eye relief have a linear relationship once the viewpoint is fixed, and the corresponding FOV can also be calculated easily. Results are plotted in Figure 4. In the system design, we would like to have a large FOV and reasonable eye relief. Therefore, we make the eye relief to be 15 mm, and the corresponding FOV of the central viewpoint is about  $55^\circ$  and the lens diameter is 15.6 mm. In this condition, the central off-axis CLC lens has an  $f$ -number of 0.96.

We have simulated the proposed system in the LightTools as Figure 5A depicts. In the simulation, we simplify the human eye as a sphere receiver (retina) and an ideal lens (pupil lens). The optical combiner consists of three reflective off-axis lenses. The off-axis angle is  $60^\circ$ ,  $44^\circ$ , and  $76^\circ$ , which corresponds to  $0^\circ$ ,  $+16^\circ$ , and  $-16^\circ$  gaze direction, respectively, since we apply an ideal lens in the optical combiner, whose focal plane is an ideal plane, even when the beam has a large incident angle. Therefore, we can see that the effective focal length of the ideal lens is angle dependent. If we set the focal length of the ideal lens as  $f$ , then the focal length is  $2f$  when the incident angle is  $60^\circ$ , and the effective focal length of the

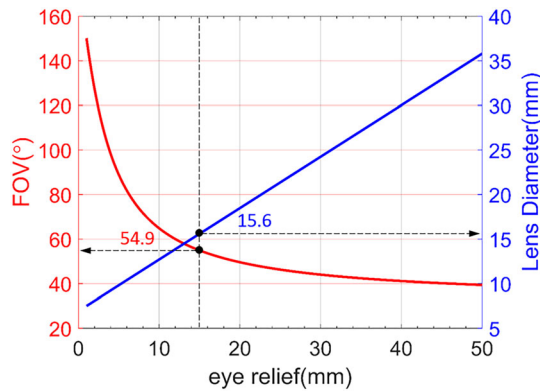


FIGURE 4 Relationship between eye relief and central FOV and lens diameter

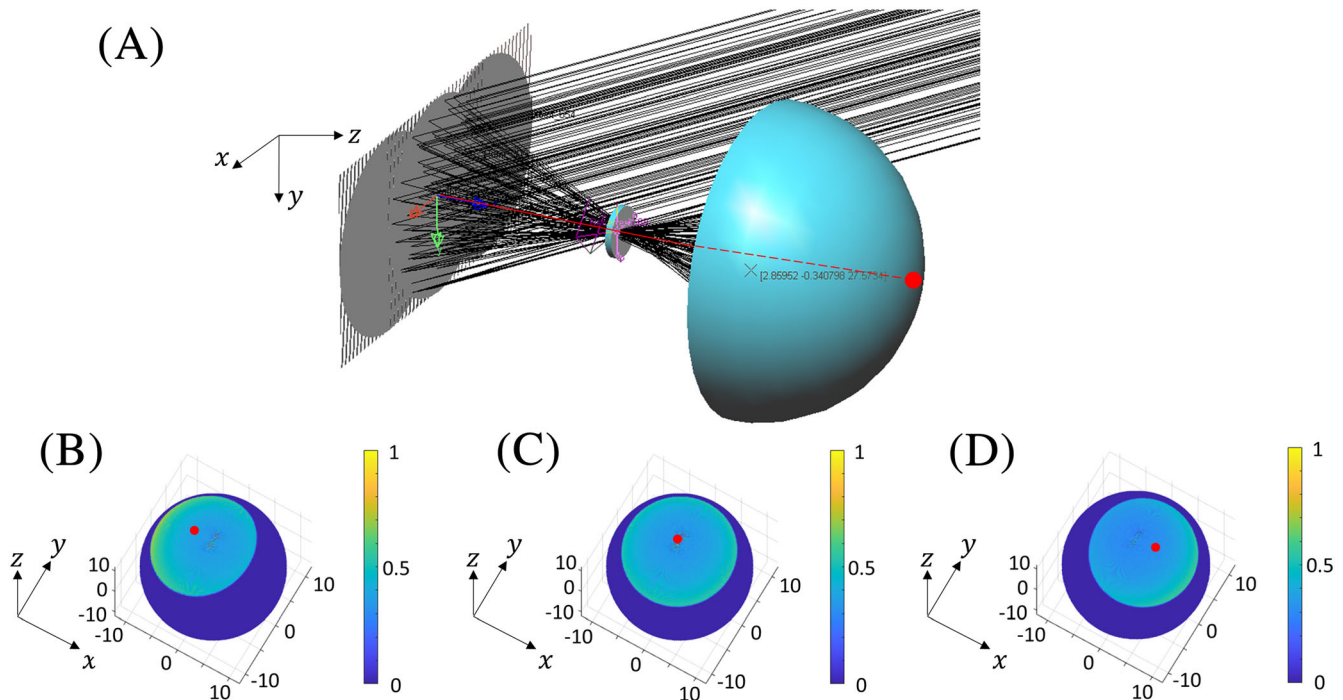


FIGURE 5 System simulation with LightTools (A) system profile, (B–D) simulation results of the signal intensity distribution on the retina with the “gaze point” (red point), when the gaze direction is  $-16^\circ$ ,  $0^\circ$ , and  $+16^\circ$ , respectively

reflective off-axis lens is  $\frac{1}{\frac{1}{f} + \frac{1}{f}} = \frac{2}{3}f$ . Since the eye relief of the system is set at 15 mm, the effective focal length of the central off-axis lens should be 15 mm, and the focal length of the ideal lens is set at 22.5 mm in the simulation. The other two off-axis lenses on the combiner should have a little bit different effective focal length, 16.09 mm, which can be easily calculated by the geometric relationship. In Figure 5A, the red line indicates the gaze direction, and the red point on the retina is the “gaze point,” which always locates at the center of the retina, no matter where the gazing direction is. Figure 5B–D shows the simulation results of the signal intensity distribution on the retina, when the gaze direction is  $-16^\circ$ ,  $0^\circ$ , and  $+16^\circ$ , respectively. We can see that the center of the FOV always match with the “gaze point,” which means the imaging content is located at the center of retina and the observer will have a natural viewing experience. These results also prove the feasibility of the proposed system.

### 3 | EXPERIMENT

#### 3.1 | Device fabrication

In experiment, we fabricated three off-axis CLC lenses. Two of them have right-handed helical structure, which works for RCP, and the other one has left-handed helical

structure, which works for LCP. The off-axis CLC lenses working for the same kind of circular polarized light are fabricated on the same substrate. The fabrication process can be found in Yin et al.<sup>16</sup> Figure 6A shows the transmission spectra of these two fabricated samples. The inputs are the specified circularly polarized light with  $60^\circ$  incident angle. From Figure 6A, the diffraction efficiency of these two samples at the operation wavelength (457 nm) is 98% and 91%, respectively. The photos of the samples are shown in Figure 6B,C. The first sample works for LCP, which corresponds to the central viewpoint. The second sample diffracts RCP and contains two off-axis lenses, corresponding to  $+16^\circ$  and  $-16^\circ$  viewpoints, respectively.

#### 3.2 | Results and discussion

We assembled the fabricated optical combiner in the system, which is depicted in Figure 7A. A laser projector (Sony MP-CL1A) was used as light engine and a bandpass filter (THROLABS FB457.9-10) was added to lower the beam intensity so that the signal at the exit pupil would not be too strong to saturate the camera. Figure 7B shows the spectra of the laser projector and bandpass filter. Only 0.43% of the laser output can pass through the bandpass filter. Two layers of the fabricated off-axis CLC lenses are laminated to form the optical combiner. The

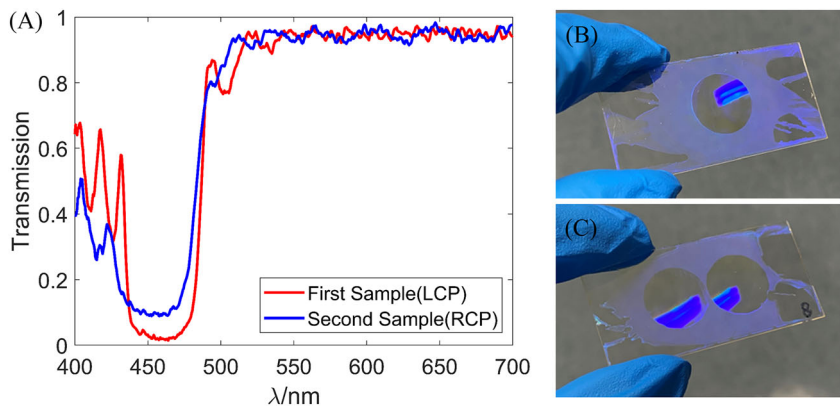


**FIGURE 6** (A) Measured transmission spectra of the fabricated samples with  $60^\circ$  incident angle and specified LCP and RCP beams. Photos of the fabricated samples working for (B) LCP and (C) RCP

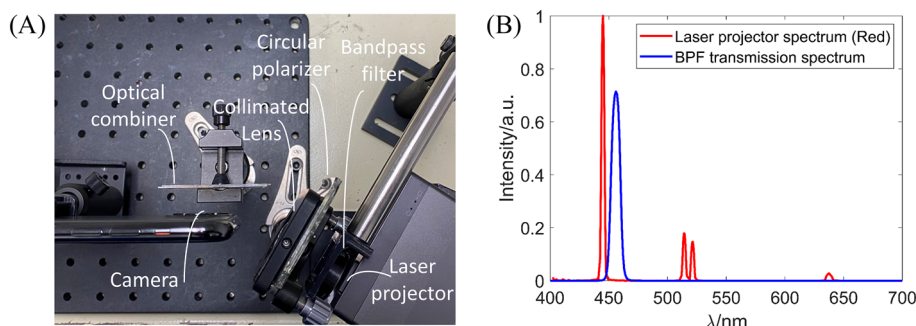


**FIGURE 7** (A) AR system setup. (B) Measured laser projector emission spectrum (red line) with only blue signal input and transmission spectrum (blue line) of bandpass filter (BPF)



imaging results are captured by a smartphone camera (iPhone 11 pro Max).

Figure 8 presents the imaging results of the three viewpoints. Figure 8A–C indicates the position of the focal points. In experiment, we placed a rod with 2.4 cm diameter at the central viewpoint to represent the user's eyeball. According to the photos, we can see that the focal points are located at the desired position on the “eyeball.” Figure 8D–F shows the imaging results with gaze direction at  $+16^\circ$ ,  $0^\circ$ , and  $-16^\circ$ , respectively. From the photos, the imaging contents are located at the center of the FOV, and the image chief ray directions are matched with the gaze direction. Moreover, the imaging FOV is also consistent with the calculation result. In addition, these off-axis lenses are recorded independently with different holographic lens patterns, and each one is optimized for the designed viewing angle and incident angle. Therefore, they will not introduce significant aberration when the beam steers. All the imaging results present good quality, and no noticeable ghost and scattering are observed.

During the photos capturing, the cellphone camera would automatically balance the intensity between ambient light and signal, so the ambient light intensity is not

the actual condition in Figure 8. To give a more direct vision of the ambient light transmittance, we present the real environment with and without the optical combiner in Figure 9. In Figure 9B, more yellowish color appears on the left, which is due to the angular dependence of the off-axis CLC lenses<sup>17</sup> (only the  $60^\circ$  incidence has the highest diffraction efficiency in our case). To improve the ambient light transmittance, the diffraction efficiency of the off-axis CLC lenses can be reduced. Although it will lead to a lower optical efficiency for the signal, the imaging intensity of Maxwellian display will not be a problem, and the signal light leakage is not noticeable. On the other hand, using a low birefringence reactive mesogen monomer to narrow the Bragg reflection band of the off-axis CLC lenses also helps to enhance the ambient light transmittance, and it will not influence the signal beam.<sup>18</sup> Moreover, the alignment layer material we used is brilliant yellow, which appears yellowish, and it also contribute slightly to the yellowish color for the whole image. If a transparent photo-alignment material was applied, then the yellowish background can be relieved.<sup>19</sup>

In this work, we have demonstrated the expanded eyebox in one dimension, while the proposed concept is



**FIGURE 8** (A–C) Photos of the focal point positions on the eyeball surface and (D–F) corresponding imaging results and gaze directions

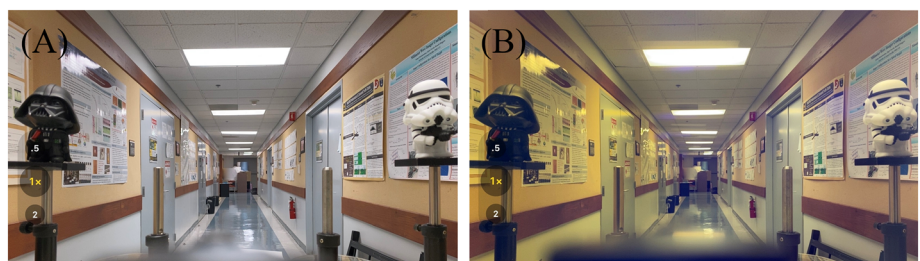


**FIGURE 9** Photos of environment background (A) without and (B) with optical combiner

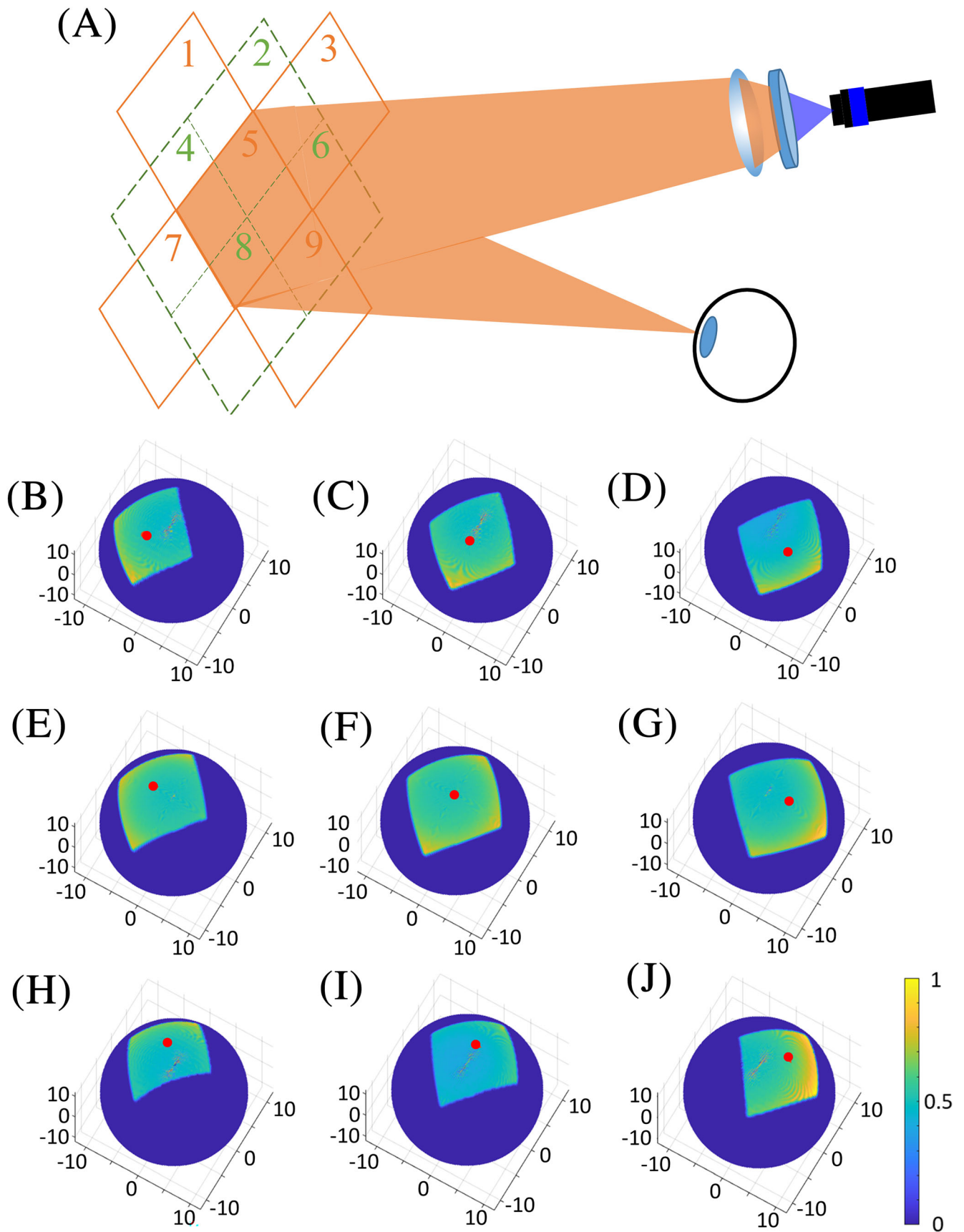


**FIGURE 10** (A) Schematic of the proposed system with 2D eyebox expansion, (B–J) simulation results of the signal intensity distribution on the retina with the “gaze point” (red point), corresponding to different off-axis lenses 1–9

also applicable to the two-dimensional (2D) eyebox expansion. The system schematic is depicted in Figure 10A. To make use of the space on the substrate with a higher efficiency, the shape of the off-axis lenses is intentionally designed to be a square in 2D eyebox expansion. In total, nine viewpoints are generated. The first layer works for LCP with five off-axis CLC lenses, and the second layer has four off-axis CLC lenses, which are working for RCP. Figure 10B–J shows the simulation results corresponding to the viewpoints of off-axis lenses from 1 to 9 in Figure 10A. From the simulation results, the signal chief rays are matched with gaze directions at all the viewpoints, which means our design is feasible for 2D eyebox expansion. It should be mentioned that in experiment, a monochromatic optical combiner was used, just to validate the proposed structure. For practical applications, multiple layers of off-axis CLC lenses can be stacked together to form a full-color optical combiner.

## 4 | CONCLUSION

We demonstrate a new pupil steering Maxwellian-view AR system structure, and the concept is validated experimentally. Besides eyebox extension, the proposed system also has advantage in gaze matching for each viewpoint, which promises a natural viewing experience. Moreover, each viewpoint is generated by one independent off-axis CLC lens so that each lens can be customized to achieve an optimal imaging quality for the corresponding viewpoint. Moreover, the system also exhibits high optical efficiency, relatively large FOV, good ambient light transmittance, compact size, and lightweight. In the system, the optical combiner consists of multiple polarization selective off-axis CLC lenses, which are fabricated by the holographic method. The fabricated off-axis CLC lenses have a large off-axis angle ( $60^\circ$ ) and low  $f$ -number (0.96), and the diffraction efficiency can be as high as 98%. The proposed pupil steering system overcomes a critical technical barrier, and its widespread applications for AR systems are foreseeable.

## ACKNOWLEDGMENTS

The authors are indebted to Goertek Electronics for the financial support and Jianghao Xiong, En-Lin Hsiang, and Tao Zhan for their stimulating discussions.

## ORCID

Junyu Zou  <https://orcid.org/0000-0001-5218-3249>

Shin-Tson Wu  <https://orcid.org/0000-0002-0943-0440>

## REFERENCES

- Furness TA, Kollin JS. Virtual retinal display. U.S. Patent 5,467,104; 1995.
- Ando T, Yamasaki K, Okamoto M, Shimizu E. Head-mounted display using a holographic optical element. *Practical Holography XII* 1998;3293:183–9. SPIE.
- Ando T, Yamasaki K, Okamoto M, Matsumoto T, Shimizu E. Retinal projection display using holographic optical element. *Practical Holography XIV and Holographic Materials VI*. 2000; 3956:211–6. SPIE.
- Kramida G. Resolving the vergence-accommodation conflict in head-mounted displays. *IEEE Trans vis Comput Graph*. 2015; 22:1912–31.
- Zhan T, Xiong J, Zou J, Wu ST. Multifocal displays: Review and prospect. *PhotonIX*. 2020;1(1):1–31.
- Lin T, Zhan T, Zou J, Fan F, Wu ST. Maxwellian near eye display with an expanded eyebox. *Opt Express*. 2020;28(26): 38616–25.
- Shrestha PK, Pryn MJ, Jia J, et al. Accommodation-free head mounted display with comfortable 3D perception and an enlarged eye-box. *Research*. 2019;2019:9273723.
- Chang C, Cui W, Park J, Gao L. Computational holographic Maxwellian near-eye display with an expanded eyebox. *Sci Rep*. 2019;9(1):18749.
- Zou J, Li L, Wu ST. Gaze-matched pupil steering Maxwellian-view augmented reality display with large angle diffractive liquid crystal lenses. *Adv Photonics Res*. 2022;3:2100362.
- Xiong J, Li Y, Li K, Wu ST. Aberration-free pupil steerable Maxwellian display for augmented reality with cholesteric liquid crystal holographic lenses. *Opt Lett*. 2021;46(7): 1760–3.
- Kim J, Jeong Y, Stengel M, et al. Foveated AR: Dynamically-foveated augmented reality display. *ACM Trans Graph*. 2019; 38(4):99.
- Xiong J, Hsiang EL, He Z, Zhan T, Wu ST. Augmented reality and virtual reality displays: Emerging technologies and future perspectives. *Light Sci Appl*. 2021;10:216.
- Xiong J, Yin K, Li K, Wu ST. Holographic optical elements for augmented reality: Principles, present status, and future perspectives. *Adv Photonics Res*. 2021;2:2000049.
- Jo Y, Yoo C, Bang K, Lee B, Lee B. Eye-box extended retinal projection type near-eye display with multiple independent viewpoints. *Appl Optics*. 2021;60(4):A268–76.
- Ratnam K, Konrad R, Lanman D, Zannoli M. Retinal image quality in near-eye pupil-steered systems. *Opt Express*. 2019; 27(26):38289–311.
- Yin K, He Z, Wu ST. Reflective polarization volume lens with small  $f$ -number and large diffraction angle. *Adv Opt Mater*. 2020;8(11):2000170.
- Lee YH, Yin K, Wu ST. Reflective polarization volume gratings for high efficiency waveguide-coupling augmented reality displays. *Opt Express*. 2017;25(22):27008–14.
- Zou J, Hsiang EL, Zhan T, Yin K, He Z, Wu ST. High dynamic range head-up displays. *Opt Express*. 2020;28(16): 24298–307.
- Guo Q, Srivastava AK, Chigrinov VG, Kwok HS. Polymer and azo-dye composite: A photo-alignment layer for liquid crystals. *Liq Cryst*. 2014;41(10):1465–72.



## AUTHOR BIOGRAPHIES



**Junyu Zou** received his B.S. in Optical Information Science and Technology from Beijing Institute of Technology and M.S. in Electrical and Computer Engineering from University of Michigan–Ann Arbor. He is currently working toward his Ph.D. degree at College of Optics and Photonics, University of Central Florida. His research interests include augmented reality and virtual reality, novel liquid crystal devices, head-up display, and holography systems.



**Zhenyi Luo** received his B.S. from the Department of Precision Instrument at Tsinghua University and M. S. from the Department of Chemistry at the University of Tokyo. He is currently working toward his Ph.D. degree at College of Optics and Photonics, University of Central Florida. His research interests include advanced augmented reality and virtual reality displays, and novel liquid crystal devices.



**Shin-Tson Wu** is a Pegasus professor at College of Optics and Photonics, University of Central Florida. He is the recipient of Optica/IS&T Edwin Land medal (2022), SPIE Maria Goeppert Mayer award (2022), OSA Esther Hoffman

Beller medal (2014), SID Slottow-Owaki prize (2011), OSA Joseph Fraunhofer award (2010), SPIE G. G. Stokes award (2008), and SID Jan Rajchman prize (2008). In 2014, he was inducted to the inaugural Florida Inventors Hall of Fame. He is a Charter Fellow of the National Academy of Inventors and a Fellow of the IEEE, OSA, SID, and SPIE. In the past, he served as founding Editor-In-Chief of the IEEE/OSA *Journal of Display Technology*, OSA Publications Council Chair, OSA Board of Directors, and SID honors and awards committee chair.

**How to cite this article:** Zou J, Luo Z, Wu S-T. Pupil steerable Maxwellian AR display with gaze matching. *J Soc Inf Display*. 2022. <https://doi.org/10.1002/jsid.1119>